

## **Bound chloride and free Cl/OH thresholds for corrosion initiation in alkali-activated concrete**

OJEDOKUN, Olalekan <<http://orcid.org/0000-0002-9573-4976>> and MANGAT, Pal <<http://orcid.org/0000-0003-1736-8891>>

Available from Sheffield Hallam University Research Archive (SHURA) at:

<https://shura.shu.ac.uk/35702/>

---

This document is the Accepted Version [AM]

**Citation:**

OJEDOKUN, Olalekan and MANGAT, Pal (2025). Bound chloride and free Cl/OH thresholds for corrosion initiation in alkali-activated concrete. Proceedings of Institution of Civil Engineers: Construction Materials. [Article]

---

**Copyright and re-use policy**

See <http://shura.shu.ac.uk/information.html>

# **Bound chloride and free Cl/OH thresholds for corrosion initiation in alkali activated concrete**

Olalekan O. Ojedokun and P.S. Mangat

Centre for Infrastructure Management, Materials and Engineering Research Institute, Sheffield Hallam  
University, Sheffield S1 1WB, UK

## **ABSTRACT**

The paper presents results of hydroxyl ion (OH) and chloride (Cl) concentrations in the pore fluid of alkali activated concrete (AAC) and their effect on steel reinforcement corrosion up to 1750 days of chloride exposure. A higher OH and corresponding lower Cl/OH was observed in AAC than the control Portland cement (PC) concrete at early ages of chloride exposure. A reversed trend was observed under long term chloride exposure for AAC and PC concrete due to the superior chloride binding capacity of Portland cement. The critical threshold Cl/OH ratio is between 2 and 3.28 for corrosion initiation in AAC, whereas it is  $< 1$  for PC concrete. Also, the critical bound chloride threshold for corrosion initiation in AAC is between 14.7 mg/g (1.47%) and 17.7 mg/g (1.77%) compared with 4 mg/g (0.4%) by binder weight for PC concrete. The steel reinforcement in AAC remains free from chloride induced corrosion for a longer period and up to higher Cl-/OH- ratios than PC concrete due to the presence of elemental Sulphur (sulfides) on the steel surface in AAC.

*Keywords: Alkali activated concrete (AAC); chloride diffusion; reinforcement corrosion; Cl-/OH- ratio; bound chloride; UN SDG 9; UN SDG 11; UN SDG 12; UN SDG 13*

## 1.0 INTRODUCTION

The hydrated products of PC concrete produce saturated pore solution containing calcium hydroxide  $\text{Ca(OH)}_2$  and different ions depending on the type of cement and supplementary cementitious materials like fly ash, slag and silica fume (Ghods *et al.*, 2009). These ionic species are principally alkali oxides of calcium, sodium and potassium in the cement component unlike AAC. Sulphate ions could also be present in the concrete pore solution due to gypsum added during cement production or from contaminated aggregate or mixing water (Neville, 2011). The pH of PC concrete pore solution increases from about 12.5 to 13.5 by the presence of these alkali oxides ( $\text{Na}^+$  and  $\text{K}^+$ ) (Angst *et al.*, 2009; Poursaeed and Hansson, 2009). However, the pH decreases when mineral admixtures are added (Neville, 2011). For example, a 10% replacement of PC cement with silica fume reduced the pH of the concrete pore solution from 13.5 to 12.6 (Ortolan, Mancio and Tutikian, 2016). This is due to the secondary pozzolanic reactions of the supplementary cementitious material which requires calcium hydroxide  $\text{Ca(OH)}_2$  from the concrete pore solution to activate these reactions. For a fly-ash based system, the glassy material is only activated when the pH of the concrete pore solution is about 13.2 (Neville, 2011) but for ground granulated blast-furnace slag (GGBS), the glassy material is activated at a lower pH of about 11.5 (Song and Jennings, 1999). Information on the chemistry of AAC pore solution is limited in literature unlike that of PC concrete pore solution which is fairly-well documented. The expectation of the chloride/hydroxyl ion ratio and its threshold value being significant in initiating and controlling corrosion in AAC requires understanding and definition. The results will elucidate the effect of alkalinity and  $\text{Cl}^-/\text{OH}^-$  ratio on the corrosion resistance of reinforcing steel in AAC.

The pH of PC concrete pore solution at considerably low values less than 12 is suggested to aid the participation of bound chloride in the corrosion initiation in reinforced concrete (Glass

and Buenfeld, 2000). It was argued that a low pH favours the dissolution of chloride ions that are physically or chemically bound to the hydration products thereby increasing the free chloride content in concrete (Page and Vennesland, 1983). Contrary to the dissolution of bound chlorides into the pore solution at low pH when the source chloride is NaCl, *Robert* (Roberts, 1962) observed the solubility of Friedel's salt at high pH when the chloride source is from CaCl<sub>2</sub>. The chemically bound chloride concentrations are released into the concrete pore solution at high pH. The difference in dissolution of bound chloride into the concrete pore solution at various pH for samples containing NaCl and CaCl<sub>2</sub> could be attributed to the solubility of their cations at various pH values (Tritthart, 1989). The effect of pH on the bound chloride solubility in the concrete pore solution is, therefore, greatly influenced by the source chloride. NaCl is used as the source chloride for this study. Recent investigation on the chloride binding capacity of alkali activated concrete shows that PC concrete had better chloride binding capacity than AAC due to its effective binding capacity in both the physically and chemically bound chlorides whereas the AAC is effective in binding only the physically bound chlorides while the chemically bound chloride is limited (Mangat and Ojedokun, 2019).

Hydroxyl ion concentration is as important as the chloride concentration in the pore solution of concrete because of its influence on corrosion rate of steel in concrete (Neville, 2011). There is the possibility of depassivation of steel embedded in concrete with an increase in the chloride/hydroxyl ion concentrations, although no valid conclusion exists on its threshold value. However, the threshold value of 0.61 for the chloride/hydroxyl ion concentration proposed by *Hausmann* (Hausmann, 1967) for the initiation of corrosion in cement-based materials does not normally apply. For example, *Lambert et al.* (Lambert, Page and Vassie, 1991) presented a chloride/hydroxyl concentration threshold of 3 for steel rods embedded in concrete. The chloride/hydroxyl concentration as high as 320 did not result in corrosion of steel

fibres embedded in fly-ash concrete (Mangat and Gurusamy, 1988). Similarly high threshold value of chloride/hydroxyl concentration in silica fume concrete was observed by *Page and Havdahl* (Page and Havdahl, 1985) for corrosion initiation. The reasons attributed to such high values were the lower chloride binding and pH which increases the  $\text{Cl}^-/\text{OH}^-$  ratio in its pore solution. *Hausmann* (Hausmann, 1967) based the chloride/hydroxyl concentration threshold of 0.61 on an idealized solution to represent the pore solution of hydrated cement. This model electrolyte cannot simulate an oxygen depletion or limited mobility of chloride ions within the cement matrix unlike the concrete pore solution (Page and Vennesland, 1983). This makes it unreliable for predicting corrosion behaviour of steel in concrete. The threshold of chloride/hydroxyl ion concentrations in AAC is expected to be different from PC concrete because of the differences in the compositions of their pore solutions.

Electrochemical reaction at the steel-concrete interface of AAC is influenced by sulfide in the pore solution of the concrete (Mangat, Ojedokun and Lambert, 2021). Oxidation reaction is delayed by sulfide deposits on the steel surface to a certain extent which reduces the rate of corrosion reaction of the embedded steel (Criado and Provis, 2018). Furthermore, elemental sulfur produced from oxidized high concentration of sulfide accumulates at the depleted passive film resulting in its repair (Ma *et al.*, 2016; Criado and Provis, 2018). Conversely, the disintegration and reduction of the passive film was observed due to the attraction of sulfide by magnetite and promoting higher corrosion rates in AAC (Tromans, 1980; El Haleem and El Aal, 2008). Blast furnace slag has high sulfide content which produces redox potentials of negative values compared to PC concrete (Ma *et al.*, 2016). Therefore, the corrosion behaviour of AAC is expected to be significantly different from PC concrete. The corrosion initiating relationship between the free chloride and pH of pore solution in AAC is not established in

literature. This paper will address the relationship between the two parameters as well as their relationship with bound chlorides.

## **2.0 EXPERIMENTAL PROGRAMME**

### **2.1 Materials and mixes**

AAC 1, 2 and 3 mixes and conventional PC concrete were produced as shown in Table 1. Ground granulated blast furnace slag (GGBS) and CEM 1 cement of grade 42.5R [8] were used as binders in AAC and PC concrete mixes respectively. The chemical composition of GGBS and CEM 1 cement is given in Table 2. Sodium silicate solution of 6.5mol/L molarity and 2% modulus, together with NaOH was used as liquid activator. The liquid activator was further diluted with 0%, 3.88% and 7.76% water to produce high (AAC 1), medium (AAC 2) and low (AAC 3) strength grades respectively as shown in Table 1 (Mangat and Ojedokun, 2019). In addition to the high (70 MPa), medium (55 MPa) and low (40 MPa) strength grades achieved using 0%, 3.88% and 7.76% respectively, AAC 1, 2 and 3 mixes were produced to determine the effect of activator dilution on chloride and hydroxyl ion concentrations. A liquid-binder ratio of 0.47, 10mm uncrushed gravel, 6mm limestone and a medium grade sand with 80% particle size passing 1mm sieve were used in both the AAC and PC concrete mixes. The properties and oxide compositions of these aggregates conform to BS 882:1992 [24]. The selected AAC and PC concrete mix parameters such as liquid to binder ratio, aggregate and binder contents are derived from the authors' previous research (Mangat and Ojedokun, 2019). The authors were able to achieve a good workability of 30 mm to 75 mm which is often a challenge for AAC, compressive strengths between 45MPa to 65MPa using optimal liquid to binder ratio and desirable pore structure and durability properties such as optimal curing regime,

chloride binding, carbonation and corrosion behaviour (Ojedokun and Mangat, 2023)(Mangat and Ojedokun, 2020)(Mangat and Ojedokun, 2018).

Table 1: Composition of AAC 1, 2, 3 and control PC concrete mixes

Mix	Binder Content (%)	Fine Agg. (%)	Coarse Agg. (%)		Liquid/Binder Ratio	Activator Dilution (%)
			10mm Gravel	6mm Limestone		
AAC 1	25	18	29.3	15.7	0.47	0
AAC 2	25	18	29.3	15.7	0.47	3.88
AAC 3	25	18	29.3	15.7	0.47	7.76
Control PC	20	26	28.9	15.5	0.47(w/c)	-

Table 2: Chemical composition of CEM 1 cement and GGBS binders

Chemical component	SiO <sub>2</sub>	Al <sub>2</sub> O <sub>3</sub>	Fe <sub>2</sub> O <sub>3</sub>	CaO	MgO	K <sub>2</sub> O	Na <sub>2</sub> O	TiO <sub>2</sub>	P <sub>2</sub> O <sub>5</sub>	MnO	SO <sub>3</sub>
CEM 1 (mass %)	11.1	8.35	3.16	64.2	2.09	1.19	0.227	1.88	2.01	2.14	3.64
GGBS (mass %)	28.6	12.4	5.7	42.3	6.1	0.8	0.4	1.78	<0.1	0.3	0.08

## 2.2 AAC and PC concrete slab preparation

### 2.2.1 Plain slab preparation

The fresh AAC and PC concrete were mixed in a 150 kg capacity Cretangle mixer in accordance with BS EN 206,2014 standard. The concrete slabs were cast into polystyrene moulds of 250 x 250 x 75 mm dimensions, which were covered with polythene sheets for 24 hrs. in the laboratory ( $20 \pm 2^{\circ}\text{C}$ , 65% R.H) followed by demoulding. The hardened concrete was further cured in water ( $20 \pm 2^{\circ}\text{C}$ ) for 27days. The specimens were taken out of water after 28 days' curing period and surface dried. Two coats of bituminous paint were applied to five faces of the slabs except the bottom cast faces (250mm x 250mm) and allowed to dry for 24hrs. The slabs were immersed in 5% by weight NaCl solution to expose the uncoated face to chloride diffusion. A higher limit of 5% chloride concentration was used to promote accelerated chloride ingress through the exposed uncoated surface as specified in the standards

(NT BUILD 443, 1995; *DD CEN/TS 12390-11: Testing hardened concrete, Part 11: Determination of the chloride resistance of concrete, unidirectional diffusion*, 2010). The NaCl solution was stirred frequently and replaced every 90 days to maintain uniform concentration. Two units of 250 x 250 x 75 mm slab specimens were produced per mix making a total of eight slab specimens.

### **2.2.2 Reinforced slab preparation**

Mild steel reinforcement bars conforming to BS 4449:2005+A3:2006 [25] were embedded in AAC and PC concrete. The length and diameter of the reinforcement bars were 400 mm and 8mm respectively which was grit blasted to remove all mill scale, rust and contamination before placing triplicates inside a polystyrene mould at a cover depth of 30 mm (Fig. 1). Each polystyrene mould with the positioned triplicate steel bars was filled with concrete in three layers. The mixing, casting and placing of fresh AAC and PC concrete were carried out similar to the plain concrete slabs in Section 2.2.1. A total of eight 250 x 250 x 75 mm steel reinforced slabs were produced for the AAC and PC concrete, two specimens for each of AAC 1, 2, 3 and PC concrete. The hardened specimens were cured similar to Section 2.2.1.

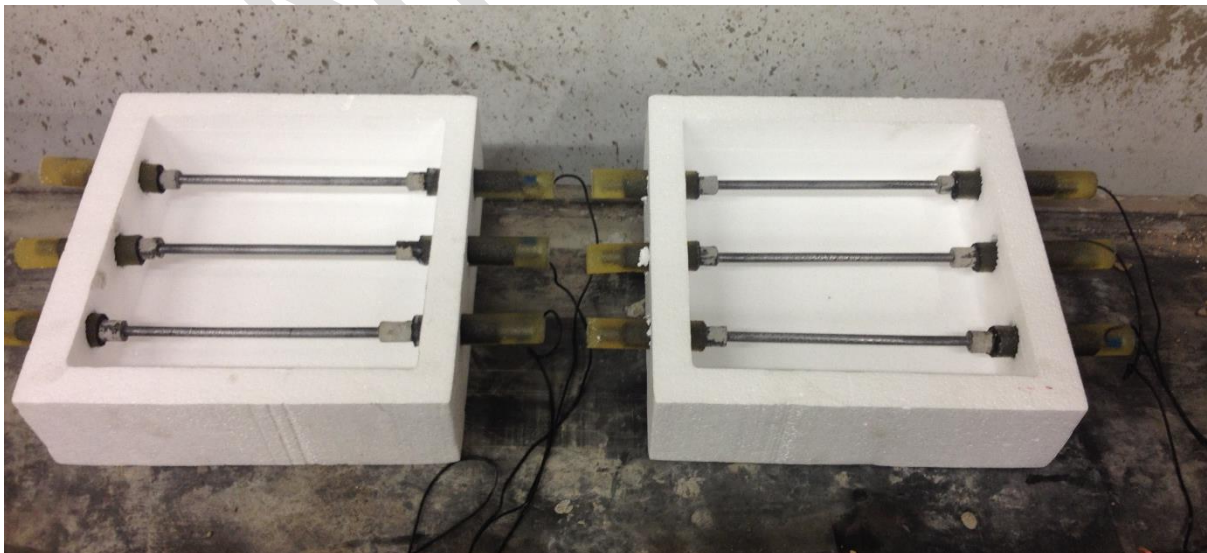


Fig. 1: Embedded Triplicate Reinforcing bars in polystyrene moulds prior to casting

### 2.3 Concrete coring and pore fluid expression

AAC and PC concrete slabs were drilled to obtain four cores of 50mm diameter x 60mm depth from each specimen as shown in Fig 2a and 2b. Three discs of 50mm diameter x 20mm depth representing depths of 0 - 20mm (10mm mean depth), 20 - 40mm (30mm mean depth) and 40 - 60mm (50mm mean depth) were obtained from each core (Fig. 2b). The pore solution was extracted by placing three 20mm thick concrete discs from the same depth into a pore fluid extraction device, for example 0 - 20mm depth obtained from three cores for each mix. The pore fluid extraction device having three concrete discs inside it was placed in a compression testing machine and a loading rate of 10kN/sec was applied (Fig. 2c). The pore fluid was extracted without allowing contact with air through suction and was immediately stored in plastic vials, labelled and sealed with parafilm. The same procedure was repeated on concrete core discs representing 20 - 40mm and 40 - 60mm depths.

The pore fluid samples were used to determine the free chloride and hydroxyl ion concentrations according to BS 1881-124:2015+A1, 2021 at 180, 270-, 540-, 860- and 1750-days exposure to the chloride solution.



Fig. 2a: Four cores obtained from each AAC and PC concrete slabs



Fig. 2b: Showing core samples of AAC (1<sup>st</sup>, 2<sup>nd</sup> from left) and PC concrete (3<sup>rd</sup>, 4<sup>th</sup> from left)



Fig. 2c: Pore fluid expression of AAC and PC concrete core discs

#### **2.4 Concrete powder sample**

Extraction of dry powder samples was carried out in accordance with the relevant standards (NT BUILD 443, 1995; *DD CEN/TS 12390-11: Testing hardened concrete, Part 11: Determination of the chloride resistance of concrete, unidirectional diffusion*, 2010). Two 250 x 250 x 75mm concrete slabs per mix at each test age were sawn into two equal halves along the plane perpendicular to the uncoated concrete face. Dry powder samples were extracted at 8, 15, 25, 35, 50 and 65mm depths from the uncoated concrete face through which chloride diffusion occurs. A minimum of six holes were drilled per depth with a hammer drill using 4mm diameter SDS drill bits. Powder samples collected at each depth were combined to provide approximately 15grams of an average sample extracted from the two slab specimens of each concrete mix. Each average powder sample from each depth was sieved through a

150 $\mu$ m sieve to obtain a finely ground sample which was carefully stored in a self-sealing plastic bag and labelled accordingly. The retained coarse material was discarded while the finer powder samples were used to determine bound chloride concentrations.

### 3.0 EXPERIMENTAL RESULTS AND DISCUSSION

#### 3.1 Free Hydroxyl concentrations

The free hydroxyl ion concentration profiles of AAC 1, 2, 3 and PC concrete at early (180 and 270 days) and later (860 and 1750 days) chloride exposure periods are shown in Figures 3 and 4 respectively. The data in Figures 3 and 4 represent mean depths from the chloride-exposed surface of 10 mm, 30 mm and 50 mm.

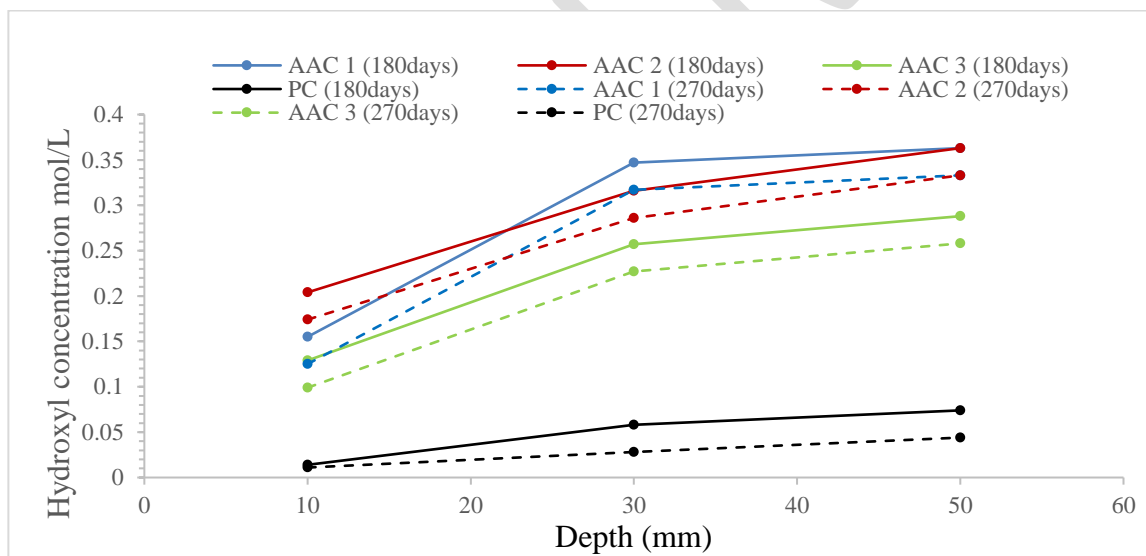


Fig. 3: Hydroxyl concentrations of AAC 1, 2, 3 and control PC concrete at 180- and 270-days exposure

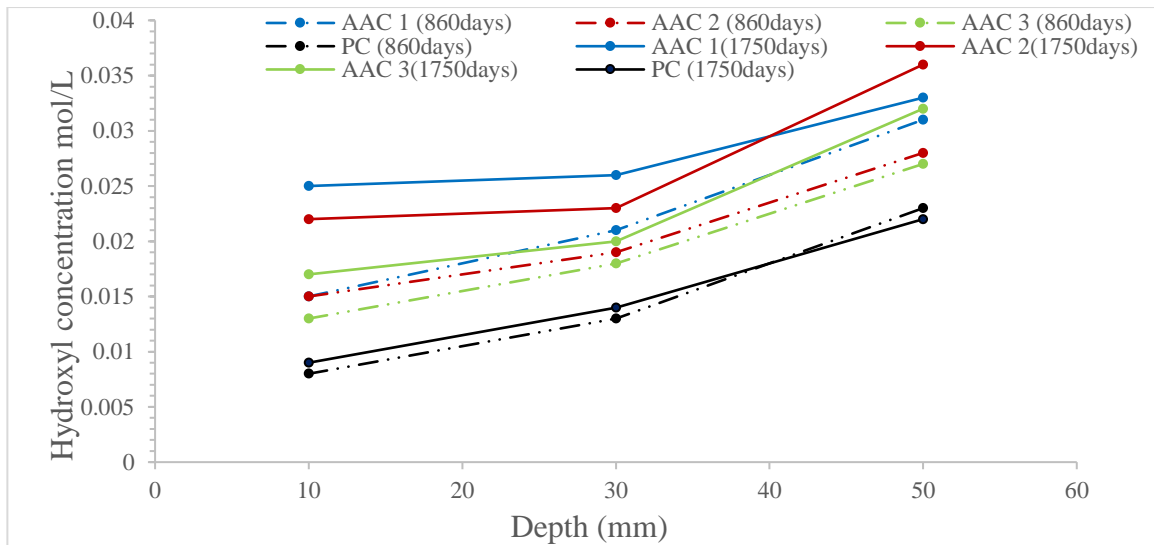


Fig. 4: Hydroxyl concentrations of AAC 1, 2, 3 and control PC concrete at 860- and 1750-days exposure

The free hydroxyl ion concentrations of all AAC mixes are very much higher than PC concrete as shown in Figure 3. The free hydroxyl ion concentrations are within the range of 0.011 mol/L to 0.074 mol/L for PC concrete compared to 0.099 mol/L to 0.363 mol/L for AAC at 180- and 270-days chloride exposure. A clear distinction in the alkalinity of AAC is amplified by the alkali activator concentration that was utilized in the AAC mixes. The alkalinity is greater at the inner core of the slab specimens. AAC 1 and 2 exhibited the highest free hydroxyl ion concentrations of 0.363 mol/L in relation to PC concrete having 0.074 mol/L at 50 mm mean depth after 180 days chloride exposure. A similar trend is observed for 270 days of chloride exposure (Fig. 3). However, the difference between free hydroxyl ion concentrations of PC relative to AAC at 860 and 1750 days in Fig. 4 is lower than at 180 and 270 days in Fig. 3. There is a notable depletion of hydroxyl ions towards the concrete surface for all profiles shown in Figures 3 and 4. The depletion is steeper between 10 mm and 30 mm depths in AAC at both 180- and 270-days chloride exposure. For example, the hydroxyl ion concentrations of AAC 1 at 180 days of exposure are 0.155 mol/L, 0.347 mol/L and 0.363 mol/L at 10 mm, 30 mm, and 50 mm depths respectively. The depletion of hydroxyl ions towards the concrete surface could

be caused by leaching of alkali content from the concrete surface (Lloyd, Provis and Van Deventer, 2010). The depletion of hydroxyl ions at the concrete surface could also be caused by the effect of carbonation. All precautions were taken to prevent carbonation which, therefore, is unlikely to be a cause of pH reduction near the surface zone. Another possible explanation for the gradual depletion of hydroxyl ions towards the concrete surface in concrete submerged in water was attributed to the outward diffusion of hydroxyl ions (Ojedokun and Mangat, 2023). Tritthart (Tritthart, 2009) proposed that under chloride exposure, competition exists between  $\text{OH}^-$  and  $\text{Cl}^-$  at the adsorption sites of hydration products. It was observed that as more chloride ions were chemically adsorbed, fewer adsorption sites were left for other ions such as  $\text{OH}^-$  which could not be absorbed simultaneously. This hypothesis was suggested as the reason for higher binding capacity for concrete with a low pH (Mangat and Ojedokun, 2020). This is unlikely for AAC because its poor binding capacity was largely due to the small amount of Friedel's salt (acid soluble chloride) or any form of crystallized salt, leaving only the kuzel's salt (water-soluble chloride) to be actively involved in the chloride binding (Ojedokun and Mangat, 2016). Luping and Nilsson (Luping and Nilsson, 1993) suggested the possibility of undissolved alkali content which is enclosed in the unhydrated slag cement to be responsible for boosting the pH of concrete pore solution especially at the inner core of concrete. AAC 2 has the highest hydroxyl ion concentration of 0.204 mol/L and 0.147 mol/L at 10 mm depth at both 180- and 270-days Cl exposure respectively but maintains the same alkalinity as AAC 1 at inner depth of 50 mm. Despite AAC 2 being 3.88% diluted with water, it produced maximum alkalinity within its pore structure relative to AAC 1 and 3. This suggests that AAC 1 has excess concentration of alkali activator which was leached into the curing solution upon sufficient wetting of its binder gel. However, the leaching was minimal at greater depths of 30 mm, showing less depletion of hydroxyl ion concentration.

### 3.2 Free chloride concentrations

The free chloride concentration profiles of AAC 1, 2, 3 and PC concrete at early (180 and 270 days) and later (860 and 1750 days) ages of chloride exposure periods are shown in Figures 5 and 6 respectively. The free chloride profiles of control PC concrete are lower than AAC 1, 2 and 3 as shown in Figures 5 and 6. For example, free chloride concentrations at 270 days exposure of AAC 1, 2, 3 and PC concrete are 0.020 mol/L, 0.023 mol/L, 0.025 mol/L, 0.022 mol/L respectively at 10 mm depth. The migration of free chloride within AAC is mainly restricted by its pore structure which is directly related to alkali activator concentration (Mangat and Ojedokun, 2018). AAC 1 with the lowest dilution of alkali activator has the lowest porosity and high volume of closed pores relative to AAC 2 and 3 concentration (Mangat and Ojedokun, 2018). These are the two distinctive pore properties that resulted in lower free chloride concentrations and have reduced the diffusion of free chloride in AAC 1 significantly.

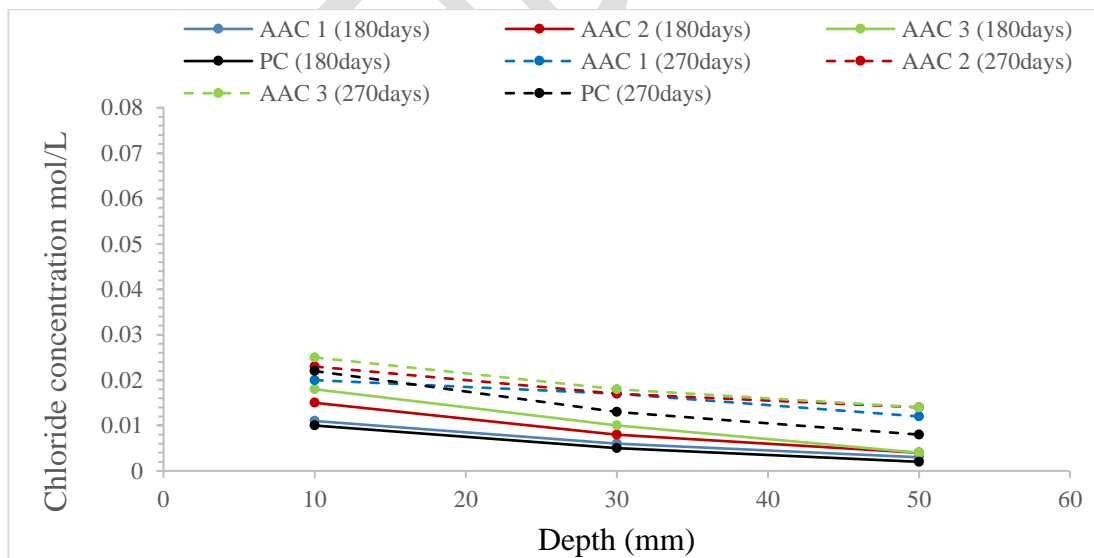


Fig. 5: Free chloride concentrations of AAC 1, 2, 3 and control PC concrete at 180- and 270-days exposure

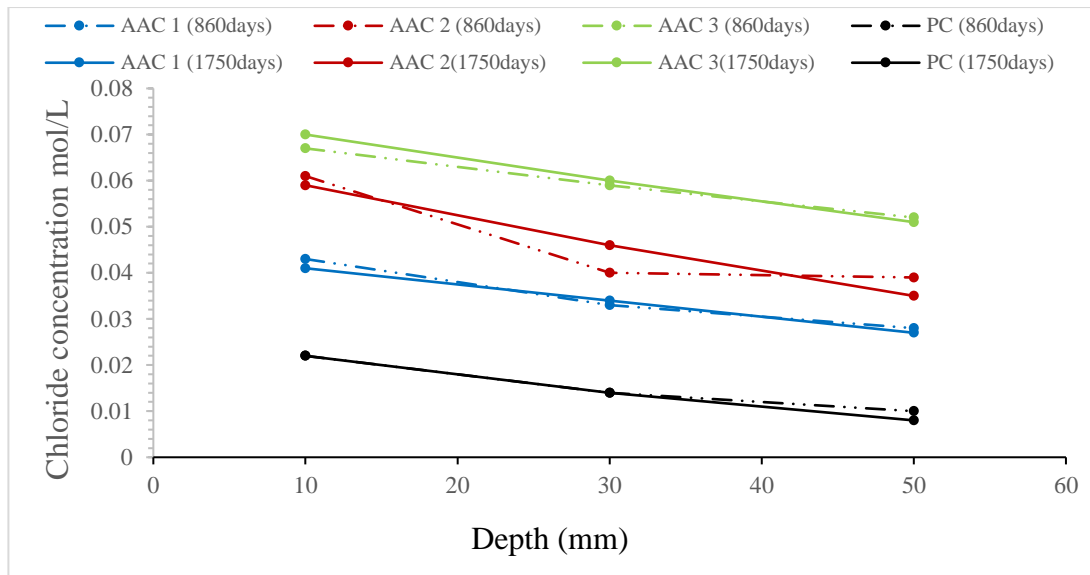


Fig. 6: Free chloride concentrations of AAC 1, 2, 3 and control PC concrete at 860- and 1750-days exposure

In addition to pore structure, the chemical and physical binding of chlorides in the PC matrix influenced the reduction of free chloride concentrations (Ojedokun and Mangat, 2016) as shown in Figures 5 and 6. Conventional PC concrete has higher total bound chloride than AAC due to the presence of C3A and C4AF in its binder. The unhydrated portion of aluminates (C3A) and aluminoferrite (C4AF) of PC binders takes up the free chloride from the concrete pore solution during the exposure period, to form Friedel's salt ( $\text{Ca}_6\text{Al}_2\text{O}_6 \cdot \text{CaCl}_2 \cdot 10\text{H}_2\text{O}$ ) and calcium chloroferrite (Sumranwanich and Tangtermsirikul, 2004). The lack of aluminates (C3A) and aluminoferrite (C4AF) in the AAC compositions results in higher free chloride concentrations in AAC. The chloride binding capacity of concrete controls its free chloride concentrations which initiate steel corrosion when their permissible limits are exceeded. There is a steep decline in the free chloride concentration from the surface to the core particularly in PC concrete at 270 days exposure. This suggests that higher chlorides are physically and chemically bound to the binder gel as they migrate towards the inner core of the concrete (Ojedokun and Mangat, 2016).

### 3.3 Free and bound Chloride Relationships

The relationships between free and bound chloride concentrations for AAC 1, 2 and 3 at 1750days were determined by non-linear regression analysis using Langmuir chloride binding isotherms in equation 1 (Luping and Nilsson, 1993; Yuan *et al.*, 2009; Thomas *et al.*, 2012). Similar relationships at early chloride exposure periods of 180, 270 and 540 days were presented elsewhere (Mangat and Ojedokun, 2020).

$$C_{tb} = (\alpha C_f)/(1 + \beta C_f) \quad 1$$

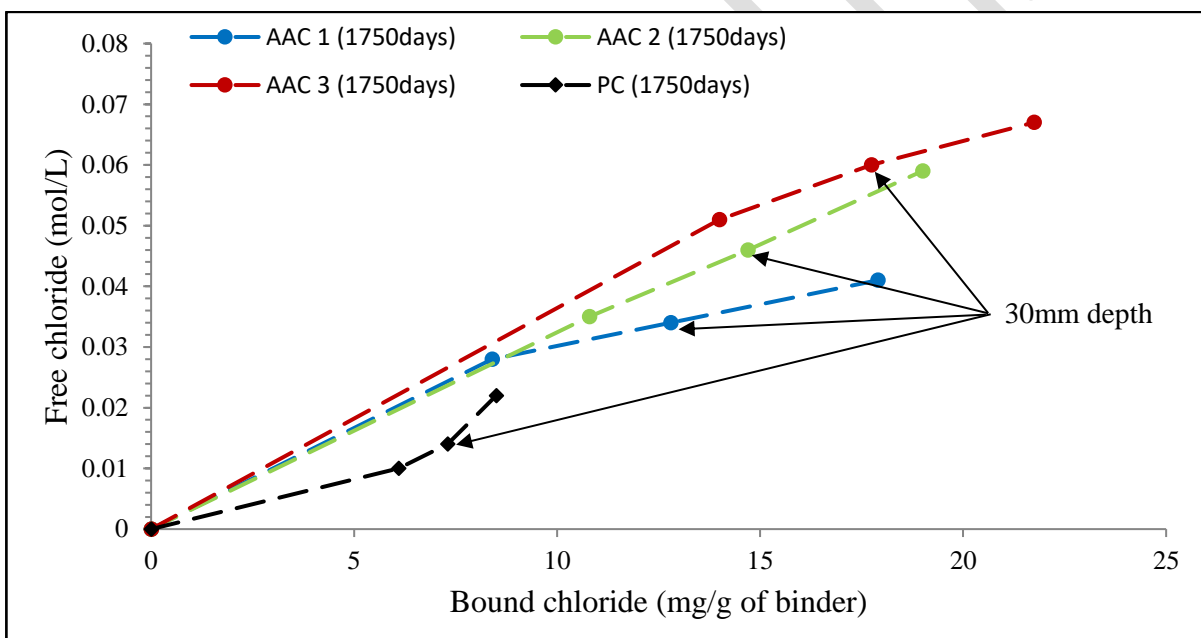


Fig. 7: Free/bound chloride relationships of AAC 1, 2 and 3 at 1750 days exposure

The maximum free chloride concentrations are 0.041mol/L, 0.059mol/L and 0.067mol/L at 10mm depth, in AAC 1, 2 and 3 respectively at 1750days of chloride exposure (Fig. 7). The free chloride concentrations in AAC 1 are less than the 0.05mol/L limit suggested by Tang and Nilsson (Luping and Nilsson, 1993) for the Langmuir isotherm to describe the effective binding of free chloride concentrations. However, the free chloride concentrations in AAC 2 and 3 are higher showing a near linear relationship with bound chloride. All adsorption sites in AAC are

likely to be occupied by chloride ions due to prolonged exposure of 1750 days thereby resulting in lower chloride concentrations in the pore solution.

BS EN 206,2014 gives a permissible bound chloride concentration of 4mg/g (0.4%) by weight of binder (cement) to prevent corrosion initiation of reinforcing steel in PC. This value relates to the acid soluble chloride determined by the tests given in international standards (NT BUILD 443, 1995; *DD CEN/TS 12390-11: Testing hardened concrete, Part 11: Determination of the chloride resistance of concrete, unidirectional diffusion*, 2010) for PC concrete. However, the bound chloride at 30mm depth, reinforcement cover depths, for AAC 1, 2, 3 and PC concrete are 12.8 mg/g (1.28%), 14.7 mg/g (1.47%) 17.7 mg/g (1.77%) and 7.3 mg/g (0.73%) by binder weight respectively as shown in Fig 7, which exceeds the permissible limit of 4mg/g (0.4%) by binder weight for PC concrete.

### **3.4 Free Chloride/ Hydroxyl ion Ratio [Cl-/OH-]**

The free chloride to hydroxyl ion concentration ratio, which is a critical threshold parameter for corrosion initiation in steel reinforcement, is shown in Figures 8 and 9 for AAC 1, 2, 3 and PC concrete at early (180 and 270 days) and later (860 and 1750 days) ages of chloride exposure periods respectively.

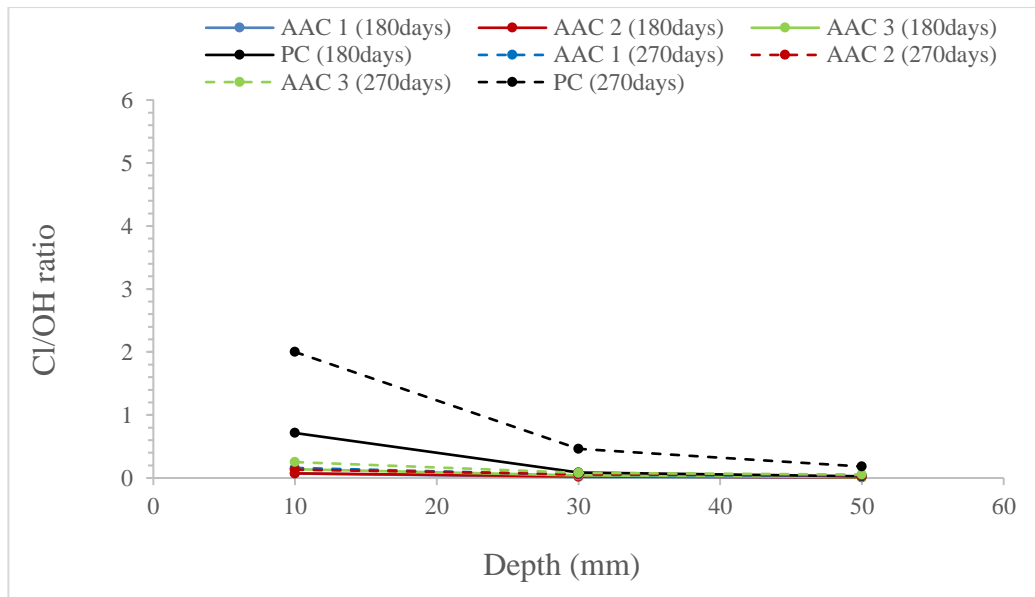


Fig. 8: Cl<sup>-</sup>/OH<sup>-</sup> ratios of AAC 1, 2, 3 and control PC concrete at 180- and 270-days exposure

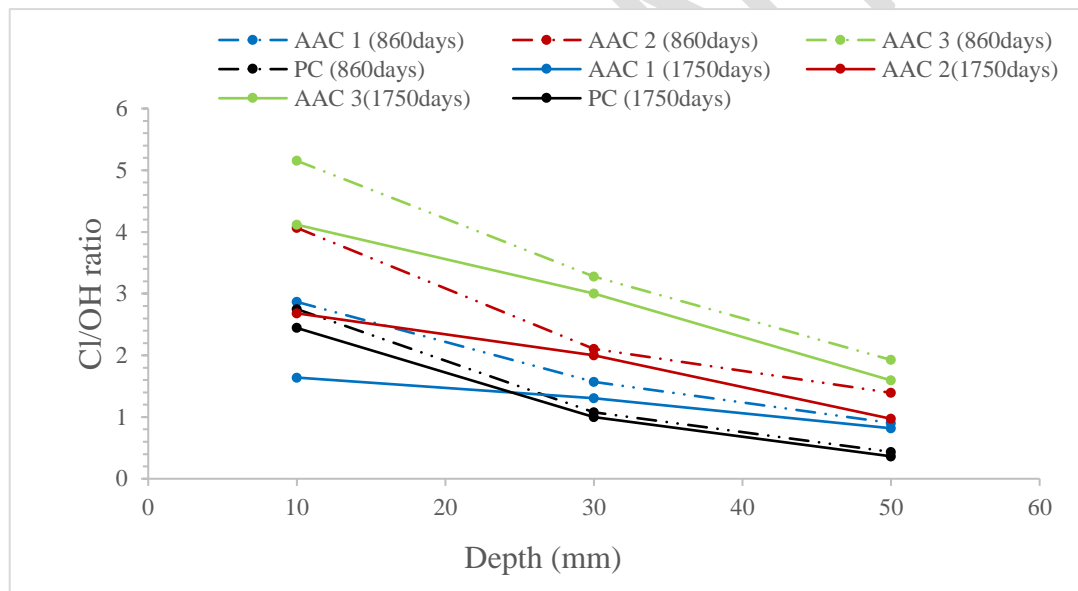


Fig. 9: Cl<sup>-</sup>/OH<sup>-</sup> ratios of AAC 1, 2, 3 and control PC concrete at 860- and 1750-days exposure

Figure 3 shows that at early age (180 and 270) days of exposure to the chloride solution, the hydroxyl ion concentration of the AAC concrete is much higher than the PC concrete while Figure 5 shows the converse result regarding chloride diffusion. The hydroxyl ion concentration dominates its influence on the Cl<sup>-</sup>/OH<sup>-</sup> ratios particularly at 270 days exposure. For example, a much lower hydroxyl ion concentration of 0.011 mol/L in PC concrete relative

to 0.099 mol/L in AAC 3 at 10 mm (Fig. 3) accounted for the much higher Cl<sup>-</sup>/OH<sup>-</sup> ratio for PC concrete than AAC 3 as shown in Fig. 8 for 270 days exposure. The hydroxyl ion concentrations in PC concrete are an order of magnitude lower than AAC 3 while the corresponding free chloride concentration is similar at 0.022mol/L and 0.025mol/L for PC and AAC 3 respectively (Fig. 5). This had significant effect on the Cl<sup>-</sup>/OH<sup>-</sup> ratios for PC concrete at 270 days which is much higher than AAC 3 at 10 mm depth (Fig. 8). Figures 4 and 6 show a reversal of the Cl<sup>-</sup>/OH<sup>-</sup> ratios with the AAC concrete having much higher values of Cl<sup>-</sup>/OH<sup>-</sup> than PC concrete, this is caused by a reduction in the differential of chloride and hydroxyl concentration between PC and AAC at the later ages due to chloride binding. A gradual decline in the Cl<sup>-</sup>/OH<sup>-</sup> ratio from 10mm to 50mm depths is observed for all AAC mixes at 180- and 270-days Cl exposure as shown in Fig. 8. The impact of low alkalinity in PC concrete relative to AAC as shown in Fig. 3 resulted in a high value of Cl<sup>-</sup>/OH<sup>-</sup> ratio. Also, a sharp decline of Cl<sup>-</sup>/OH<sup>-</sup> ratio is observed between 10mm to 30mm depths, especially in PC concrete (Fig. 8). The physical and chemical binding of free chloride, particularly for PC concrete at 30mm depth, played a major role in the reduction of Cl<sup>-</sup>/OH<sup>-</sup> ratio. The significant reduction of hydroxyl concentration particularly at 10 mm depths of PC concrete at 270 days of Cl exposure contributed significantly to the increased Cl<sup>-</sup>/OH<sup>-</sup> ratio over time. For example, the Cl<sup>-</sup>/OH<sup>-</sup> ratio at 10mm depths of AAC 1, 2, 3 and PC are 0.16, 0.13, 0.25 and 2.0 at 270 days exposure. The Cl<sup>-</sup>/OH<sup>-</sup> ratio of AAC is an order of magnitude lower than the PC concrete. The effect of high alkalinity in AAC accounts for the significant reduction in Cl<sup>-</sup>/OH<sup>-</sup> ratios.

### **3.5 Reinforcement corrosion**

The impact of Cl<sup>-</sup>/OH<sup>-</sup> ratio on the corrosion initiation of steel reinforcements in PC concrete is well documented in literature (Lambert, 2002) which is not the case for AAC. In addition to

$\text{Cl}^-/\text{OH}^-$  ratio facilitating the corrosion of steel reinforcements in AAC concrete, the presence of elemental sulfur at the steel surface has significantly impeded the propagation of corrosion (Mangat, Ojedokun and Lambert, 2021). It would have been expected that a higher corrosion activity would occur in steel reinforced AAC due to its very high  $\text{Cl}^-/\text{OH}^-$  ratios relative to PC concrete after long term chloride exposure (Figure 9). However, this is not the case as shown in Fig. 10. The  $\text{Cl}^-/\text{OH}^-$  ratios at 30 mm depth from the surface (cover provided to the reinforcement bars) in AAC 1, 2, 3 and PC concrete after 1750 days of Cl exposure are 1.57, 2, 3.28 and  $< 1$  respectively (Fig. 9). The extraction of steel reinforcements embedded at 30mm cover in AAC and PC concrete exposed to chlorides up to 1750 days revealed that ACC 1 and 2 showed no sign of corrosion activity. However, AAC 3 showed some signs of corrosion activity but much less than the PC concrete as shown in Fig. 10.

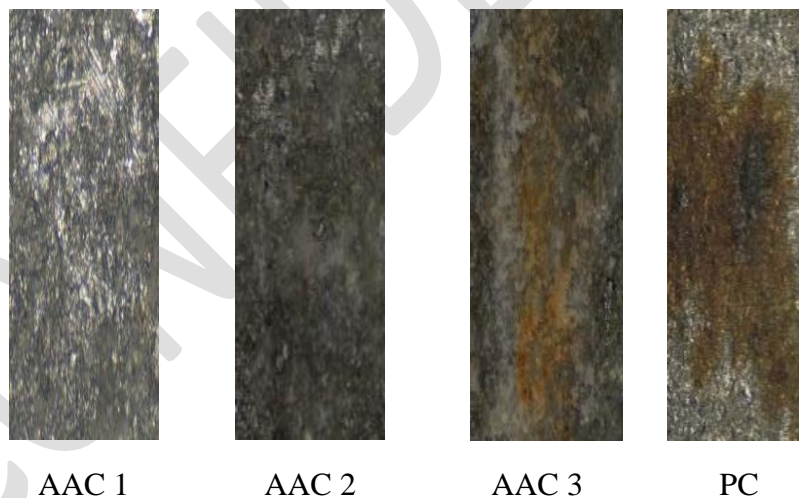


Figure 10: Corrosion of steel reinforcement in AAC, 1, 2, 3 and PC concrete after 1750 days exposure

Elemental Sulfur observed on steel reinforcements in AAC provided extra protection against corrosion activity, similar to  $\text{Ca}(\text{OH})_2$  forming a thin film around steel reinforcements in PC concrete (Mangat, Ojedokun and Lambert, 2021). The primary source of sulfur content in AAC

is from GGBS binder which reacts during geopolymerization to form various oxides such as  $\text{H}_2\text{S}$ ,  $\text{Sn}^{2-}$ ,  $\text{SO}_3^{2-}$ ,  $\text{S}_2\text{O}_3^{2-}$  and  $\text{SO}_4^{2-}$ . Elemental Sulfur decreases the amount of dissolved oxygen concentration in the pore solution of AAC leading to highly reducing redox environment (Vollpracht *et al.*, 2016). The  $\text{Cl}^-/\text{OH}^-$  ratio in PC concrete is controlled by the removal of chloride ions from the pore solution by chloride binding and simultaneously replaced by  $\text{OH}^-$  through the buffering effect of hydration product  $\text{Ca}(\text{OH})_2$ , thereby limiting absorption sites for further chloride ingress. There is no similar buffering effect in AAC, however, its corrosion activities are greatly influenced by the presence of sulfides which regulate the cathodic reaction causing steel corrosion.

Similar to  $\text{Cl}^-/\text{OH}^-$  ratio of AAC exceeding the permissible limits for PC concrete, the bound chloride at 30 mm depth is 12.8 mg/g (1.28%), 14.7 mg/g (1.47%) and 17.7 mg/g (1.77%) by binder weight for AAC 1, 2 and 3 respectively exceeding the permissible limit of 4mg/g (0.4%) by binder weight for PC concrete. No corrosion activity occurred in AAC 1 and 2 having 12.8 mg/g (1.28%), 14.7 mg/g (1.47%) by binder weight respectively. Some corrosion activity occurred in AAC 3 having 17.7 mg/g (1.77%) by binder weight and it is more pronounced in PC concrete having 7.3 mg/g (0.73%) by cement weight as shown in Fig. 10. Therefore, it can be deduced that the critical bound chloride threshold for corrosion initiation in AAC is between 14.7 mg/g (1.47%) and 17.7 mg/g (1.77%) by binder weight. Evaluating the relative performance of AAC suggests a higher permissible bound chloride concentration for corrosion initiation. No corrosion activity was observed in AAC relative to PC concrete, particularly in AAC 1 and 2. However, with varying AAC mix compositions affecting this value, a certain degree of approximation will be inevitable.

## 4.0 CONCLUSIONS

The following conclusions can be drawn from this study based on the results presented:

The hydroxyl ion concentration of AAC exposed to a 5% chloride solution is higher than PC concrete. The differential is very high at early exposure period (up to 270 days) but decreases with longer term exposure. The free chloride concentration of AAC is much higher than PC concrete due to the high chloride binding capacity of the latter. The Cl-/OH- ratios of PC concrete is higher than AAC at early periods of chloride exposure (up to 270 days) but suffer a reversal at later periods (over 560 days) due to the much higher chloride binding capacity of PC concrete. The critical threshold Cl/OH ratio for corrosion initiation in AAC is between 2 and 3.28, whereas it is  $< 1$  for PC concrete. Also, the critical bound chloride threshold for corrosion initiation in AAC is between 14.7 mg/g (1.47%) and 17.7 mg/g (1.77%) by binder weight. The Steel reinforcement embedded in AAC remains free from chloride induced corrosion for a longer period and up to higher Cl-/OH- ratios than PC concrete due to the presence of elemental Sulphur (sulfides) on the steel surface in AAC.

## ACKNOWLEDGMENTS

The authors gratefully acknowledge the continuing support of Materials and Engineering Research Institute, Sheffield Hallam University. The authors also acknowledge the award of the UK - India Newton - Bhabha award for research on AACMs.

*Please note: "For the purpose of open access, the author has applied a Creative Commons Attribution (CC BY) licence to any Author Accepted Manuscript version of this paper arising from this submission."*

## REFERENCES

- Angst, U. *et al.* (2009) 'Critical chloride content in reinforced concrete - A review', *Cement and Concrete Research*, 39, pp. 1122–1138. Available at:  
<https://doi.org/10.1016/j.cemconres.2009.08.006>.
- BS 1881-124:2015+A1 (2021) *Testing Concrete Methods for analysis of hardened concrete*.
- BS EN 206 (2014) *Concrete — Specification, performance, production and conformity*.  
British Standards Institution.
- Criado, M. and Provis, J.L. (2018) 'Alkali activated slag mortars provide high resistance to chloride-induced corrosion of steel', *Frontiers in Materials* [Preprint]. Available at:  
<https://doi.org/10.3389/fmats.2018.00034>.
- DD CEN/TS 12390-11: Testing hardened concrete, Part 11: Determination of the chloride resistance of concrete, unidirectional diffusion* (2010).
- Galan, I. and Glasser, F.P. (2015) 'Chloride in cement', *Advances in Cement Research*, 27(2), pp. 63–97. Available at: <https://doi.org/10.1680/adcr.13.00067>.
- Ghods, P. *et al.* (2009) 'The effect of concrete pore solution composition on the quality of passive oxide films on black steel reinforcement', *Cement and Concrete Composites*, 31(1), pp. 2–11. Available at: <https://doi.org/10.1016/j.cemconcomp.2008.10.003>.
- Glass, G.K. and Buenfeld, N.R. (2000) 'The influence of chloride binding on the chloride induced corrosion risk in reinforced concrete', *Corrosion Science* [Preprint]. Available at:  
[https://doi.org/10.1016/S0010-938X\(99\)00083-9](https://doi.org/10.1016/S0010-938X(99)00083-9).
- El Haleem, S.M.A. and El Aal, E.E.A. (2008) 'Electrochemical behaviour of iron in alkaline sulphide solutions', in *Corrosion Engineering Science and Technology*. Available at:  
<https://doi.org/10.1179/174327807X234769>.

- Hausmann, D.A. (1967) 'Steel corrosion in concrete -- how does it work?', *Materials Protection*, 6(11), pp. 19–23.
- Lambert, P. (2002) 'Corrosion Mechanisms – an Introduction to Aqueous Corrosion', pp. 1–5.
- Lambert, P., Page, C.L. and Vassie, P.R.W. (1991) 'Investigations of reinforcement corrosion. 2. Electrochemical monitoring of steel in chloride-contaminated concrete', *Materials and Structures*, 24(5), pp. 351–358. Available at: <https://doi.org/10.1007/BF02472068>.
- Lloyd, R.R., Provis, J.L. and Van Deventer, J.S.J. (2010) Pore solution composition and alkali diffusion in inorganic polymer cement', *Cement and Concrete Research*, 40, p. 2010. Available at: <https://doi.org/10.1016/j.cemconres.2010.04.008>.
- Luping, T. and Nilsson, L.O. (1993) 'Chloride binding capacity and binding isotherms of OPC pastes and mortars', *Cement and Concrete Research*, 23, pp. 247–253. Available at: [https://doi.org/10.1016/0008-8846\(93\)90089-R](https://doi.org/10.1016/0008-8846(93)90089-R).
- Ma, Q. *et al.* (2016) 'Chloride transport and the resulting corrosion of steel bars in alkali activated slag concretes', *Materials and Structures*, 49(9), pp. 3663–3677. Available at: <https://doi.org/10.1617/s11527-015-0747-7>.
- Mangat, P.S. and Gurusamy, K. (1988) 'Corrosion resistance of steel fibres in concrete under marine exposure', *Cement and Concrete Research*, 18(1), pp. 44–54. Available at: [https://doi.org/10.1016/0008-8846\(88\)90120-2](https://doi.org/10.1016/0008-8846(88)90120-2).
- Mangat, P.S. and Ojedokun, O.O. (2018) 'Influence of curing on pore properties and strength of alkali activated mortars', *Construction and Building Materials*, 188, pp. 337–348. Available at: <https://doi.org/10.1016/J.CONBUILDMAT.2018.07.180>.

Mangat, P.S. and Ojedokun, O.O. (2019) Bound chloride ingress in alkali activated concrete', *Construction and Building Materials*, 212. Available at:

<https://doi.org/10.1016/j.conbuildmat.2019.03.302>.

Mangat, P.S. and Ojedokun, O.O. (2020) Free and bound chloride relationships affecting reinforcement cover in alkali activated concrete', *Cement and Concrete Composites*, p.

103692. Available at: <https://doi.org/10.1016/j.cemconcomp.2020.103692>.

Mangat, P.S., Ojedokun, O.O. and Lambert, P. (2021) Chloride-initiated corrosion in alkali activated reinforced concrete', *Cement and Concrete Composites*, 115. Available at:

<https://doi.org/10.1016/j.cemconcomp.2020.103823>.

Neville, A.M. (2011) *Properties of Concrete*, Pearson Education Limited. Pearson Education Limited.

NT BUILD 443 (1995) *Concrete, Hardened: Accelerated Chloride Penetration*.

Ojedokun, O.O. and Mangat, P.S. (2016) 'Chloride diffusion in alkali activated concrete', in *II International Conference on Concrete Sustainability ICCS16, Madrid, Spain*, pp. 521–530.

Ojedokun, O.O. and Mangat, P.S. (2023) Chemical composition and physico-mechanical properties of carbonated alkali activated concrete and mortar', *Journal of Building*

*Engineering*, 71, p. 106480. Available at:

<https://doi.org/https://doi.org/10.1016/j.jobe.2023.106480>.

Ortolan, V.K., Mancio, M. and Tutikian, B.F. (2016) 'Evaluation of the influence of the pH of concrete pore solution on the corrosion resistance of steel reinforcement', *Journal of*

*Building Pathology and Rehabilitation*, 1(10), pp. 1–7. Available at:

<https://doi.org/10.1007/s41024-016-0011-8>.

- Page, C.L. and Havdahl, J. (1985) 'Electrochemical monitoring of corrosion of steel in microsilica cement pastes', *Materials and Structures*, 18(1), pp. 41–47. Available at: <https://doi.org/10.1007/BF02473363>.
- Page, C.L. and Vennesland (1983) 'Pore solution composition and chloride binding capacity of silica-fume cement pastes', *Matériaux et Construction*, 16(1), pp. 19–25. Available at: <https://doi.org/10.1007/BF02474863>.
- Poursae, A. and Hansson, C.M. (2009) 'Potential pitfalls in assessing chloride-induced corrosion of steel in concrete', *Cement and Concrete Research*, 39(5), pp. 391–400. Available at: <https://doi.org/10.1016/j.cemconres.2009.01.015>.
- Rixom, M.R. and Mailvaganam, N.P. (1986) *Chemical Admixture for Concrete*. 2nd Edition. New York: E. & F.N. Spon Ltd.
- Roberts, M.H. (1962) 'Effect of calcium chloride on the durability of pre-tensioned wire in prestressed concrete', *Magazine of Concrete Research*, 14(42), pp. 143–154. Available at: <https://doi.org/10.1680/mac.1962.14.42.143>.
- Song, S. and Jennings, H.M. (1999) 'Pore solution chemistry of alkali-activated ground granulated blast-furnace slag', *Cement and Concrete Research*, 29(2), pp. 159–170. Available at: [https://doi.org/10.1016/S0008-8846\(98\)00212-9](https://doi.org/10.1016/S0008-8846(98)00212-9).
- Sumranwanich, T. and Tangtermsirikul, S. (2004) 'A model for predicting time-dependent chloride binding capacity of cement-fly ash cementitious system', *Materials and Structures*, 37(6), pp. 387–396. Available at: <https://doi.org/10.1007/BF02479635>.
- Thomas, M.D.A. *et al.* (2012) 'The effect of supplementary cementitious materials on chloride binding in hardened cement paste', *Cement and Concrete Research*, 42, pp. 1–7. Available at: <https://doi.org/10.1016/j.cemconres.2011.01.001>.

Tritthart, J. (1989) 'Chloride binding in cement II. The influence of the hydroxide concentration in the pore solution of hardened cement pastes on chloride binding', *Cement and Concrete Research*, 19(5), pp. 683–691. Available at: [https://doi.org/10.1016/0008-8846\(89\)90039-2](https://doi.org/10.1016/0008-8846(89)90039-2).

Tritthart, J. (2009) 'Pore solution of concrete: The equilibrium of bound and free chloride', *Materials and Corrosion*, 60(8), pp. 579–585. Available at: <https://doi.org/10.1002/maco.200905277>.

Tromans, D. (1980) Anodic Polarization Behavior of Mild Steel in Hot Alkaline Sulfide Solutions', *Journal of The Electrochemical Society* [Preprint]. Available at: <https://doi.org/10.1149/1.2129865>.

Vollpracht, A. *et al.* (2016) The pore solution of blended cements: a review', *Materials and Structures/Materiaux et Constructions* [Preprint]. Available at: <https://doi.org/10.1617/s11527-015-0724-1>.

Yuan, Q. *et al.* (2009) 'Chloride binding of cement-based materials subjected to external chloride environment - A review', *Construction and Building Materials*, 23, pp. 1–13. Available at: <https://doi.org/10.1016/j.conbuildmat.2008.02.004>.